JACS
JOURNAL OF THE AMERICAN CHEMICAL SOCIETY

Communication

pubs.acs.org/JACS

A Hierarchical Self-Assembly System Built Up from Preorganized Tripodal Helical Metal Complexes

Takashi Nakamura, Hikaru Kimura, Takashi Okuhara, Masaki Yamamura, and Tatsuya Nabeshima*

Graduate School of Pure and Applied Sciences and Tsukuba Research Center for Interdisciplinary Materials Science (TIMS), University of Tsukuba, 1-1-1 Tennodai, Tsukuba, Ibaraki 305-8571, Japan

Supporting Information

ABSTRACT: The hierarchical organization strategy has realized elaborate supramolecular structures that are difficult to achieve by a one-pot thermodynamically driven self-assembly. Self-assembly via Schiff base formation of the preorganized tripodal helical unit $\mathbf{2}^{2+}$, which is composed of the tris(bipyridyl) ligand **1** and octahedral metal ion (Ru^{II} and Fe^{II}), lead to two supramolecular structures, i.e., a macrobicyclic dimer and an interlocked helicate. Notably, the interlocked helicate had a unique motif with an elongated shape (~58 Å) and linearly aligned metal centers with homochiral configurations (all-Δ or all-Λ), which shows potential for allosteric regulation based on the long-range transmittance of the structural information.

Hierarchical systems, which are constructed from small components in a multilevel manner, realize elaborate functions that are difficult to achieve with only its component.[1] Many hierarchical structures are found in living organisms both on macro and molecular scale levels. For instance, DNA, which itself is a regularly structured double-stranded helical polymer, is wrapped around histone proteins in a controlled manner and further aggregates to form chromosomes.[2] Artificial self-assembly systems are too premature to achieve such a sophisticated organization, but they are endowed with a huge potential by virtue of their designability and predictability based on chemical synthesis. Using reversible interactions between components, thermodynamically stable final products are obtained as the result of a self-error correction process.[3]

In particular, mechanically interlocked molecules[4] have attracted much attention in the field of artificial self-assembly, not only for their aesthetic appeal but also for their functions as molecular machines[5] and allosteric molecular hosts.[6,7] Catenanes, rotaxanes, and many other intertwined molecules have been reported.[8,9] For the construction of these structures, Schiff bases have been often used for their directionality, thermodynamic stability, and coordination ability of the nitrogen atoms.[10,11] Various elaborate self-assembled structures are constructed via self-assembly of metal ions, amines, and aldehydes.[12,13] The self-assembly of many components is, however, sometimes hard to design a priori, because many factors govern the process and they are prone to be affected by the synthetic conditions.

We envisioned that the use of a large, preorganized building block is a solution to predict and build up intricate yet well-defined molecular structures via hierarchical self-assembly. In this study, a helical unit composed of a tripodal ligand **1** and an octahedral metal ion (Fe^{II} or Ru^{II}) was used as a building block (Figure 1a). Our group previously reported tripodal helical

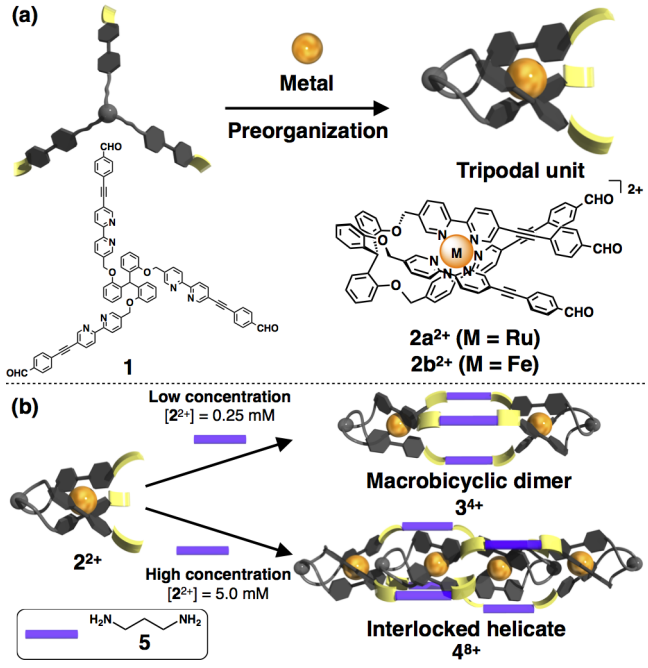

Figure 1. (a) Preorganization of a ligand **1**, bearing three bipyridyl and three formyl groups, into a tripodal helical metal complex $\mathbf{2}^{2+}$. (b) Macrobicyclic dimer $\mathbf{3}^{4+}$ and interlocked helicate $\mathbf{4}^{8+}$ self-assembled from a tripodal unit $\mathbf{2}^{2+}$ via imine bond formation with 1,3-propanediamine **5**.

pseudocryptands that regulate binding selectivity to guest molecules in response to the complexation of a metal to terminal bipyridyl groups.[14] Tripodal motives have been used as molecular receptors[15] and chelating ligands,[16] including bipyridyl-incorporated tripodands.[17] We took notice of the fact that the resultant tripodal units after complexation have rigid helical structures. With the preorganized backbone, we can geometrically design further self-assembled supramolecules based on a tripodal unit as the building block. We now report a hierarchical self-assembly system built up from the tripodal

Received: December 7, 2015
Published: January 8, 2016

DOI: 10.1021/jacs.5b12752
J. Am. Chem. Soc. 2016, 138, 794−797

metal complex $\mathbf{2}^{2+}$ bearing an aldehyde group at each toe of three "legs". Imine bond formation of the tripodal unit $\mathbf{2}^{2+}$ and 1,3-propanediamine **5** resulted in two supramolecular structures, namely, the macrobicyclic dimer $\mathbf{3}^{4+}$ and interlocked helicate $\mathbf{4}^{8+}$, depending on the concentration of the components (Figure 1b). Notably, the interlocked helicate $\mathbf{4}^{8+}$, which was built up from four tripodal units and six diamine linkers, had a unique structural motif with an elongated shape (~58 Å) and linearly aligned metal centers with homochiral configurations (all-Δ or all-Λ).

The tripodal ligand **1** consists of three parts. First, a triarylmethane group was used as a pivot part of the tripodand.[16b] Second, a 2,2′-bipyridyl group (bpy) was joined via a methyleneoxy linker on each phenyl group. During complexation with an octahedral metal ion, the three legs of **1** intramolecularly form the tris(bpy) complex. The length and substitution pattern of the pivot-linker part was designed to form a stable and fixed helical tripodal scaffold upon this preorganization. The geometric restriction only allowed the formation of a *fac*-isomer (Δ or Λ) around the metal center. Third, a formyl group was introduced to the other end of each bpy group via an ethenylphenyl linker. This long and rigid linker makes it possible to transmit the conformational change of the metal-binding bpy part to the terminal formyl group. Dynamic formation of the Schiff base with suitable polyamines to connect the molecular units bearing formyl groups results in the formation of a multicomponent self-assembled structure. In spite of its coordination ability, the resultant imine does not remove the metal ion from the bpy part, thus orthogonal structural construction is realized.

The syntheses of the tripodal ligand **1** and metal complexes **2a**·$(PF_6)_2$ (M = Ru^{II}) and **2b**·$(PF_6)_2$ (M = Fe^{II}) are described in the Supporting Information. The compounds were characterized by NMR, HR ESI-MS, UV−vis, and elemental analysis. A single crystal of **2a**·$(PF_6)_2$ suitable for X-ray diffraction analysis was obtained by slow diffusion of diethyl ether vapor into an acetonitrile solution of the complex. Figure 2 shows the

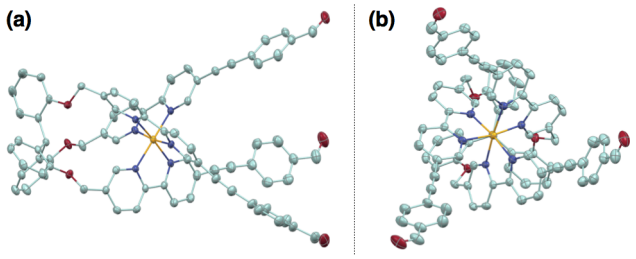

Figure 2. X-ray crystal structure of **2a**·$(PF_6)_2$. An ellipsoidal model (50% probability). Hydrogen atoms, solvents, and PF_6^- anions were omitted for clarity. C, light green; N, blue; O, red; Ru, orange. (a) Side and (b) top views.

asymmetric unit of $\mathbf{2a}^{2+}$. A Δ isomer is shown in the figure, but the complex was crystallized in the *P*-1 space group, thus there were equal numbers of Δ and Λ enantiomers within the unit cell. Three phenyl rings of the pivot part had a conformation like a propeller, and methine hydrogen pointed inward. Three legs were helically aligned around the Ru^{II} metal center and radiated outward. The terminal formyl groups were positioned relatively spaced from each other with distances between their carbon atoms in the range of 12.2−12.9 Å. Figure 3a shows the ^{1}H NMR spectrum of **2a**·$(PF_6)_2$ in $CDCl_3/CD_3CN$ = 1:1 (v/v). The benzylic protons *j* of the metal-free ligand **1** were observed as a singlet at δ = 5.04 ppm in the same solvent. In contrast, those of

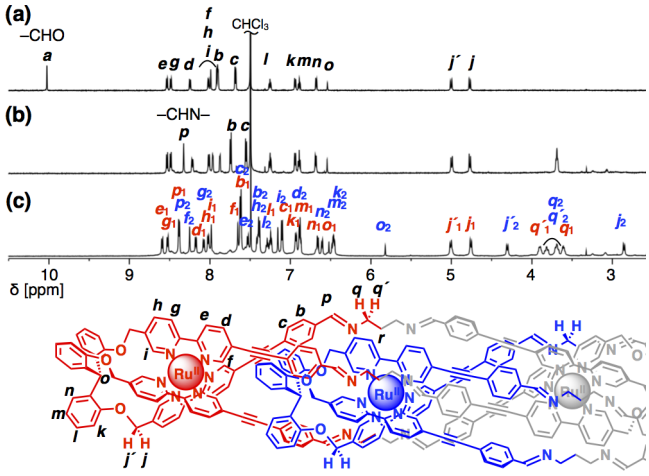

Figure 3. Formation of macrobicyclic dimer **3a**·$(PF_6)_4$ and interlocked helicate **4a**·$(PF_6)_8$ (^{1}H NMR, 600 MHz, 298 K, $CDCl_3/CD_3CN$ = 1:1). (a) Ru tripodand **2a**·$(PF_6)_2$. (b) **3a**·$(PF_6)_4$ formed from **2a**·$(PF_6)_2$ and **5** at low concentration ([**2a**·$(PF_6)_2$] = 0.25 mM). (c) **4a**·$(PF_6)_8$ formed from **2a**·$(PF_6)_2$ and **5** at high concentration ([**2a**·$(PF_6)_2$] = 5.0 mM).

the tripodal complex **2a**·$(PF_6)_2$ became diastereotopic and observed as two doublets (δ = 5.00, 4.77 ppm (J = 10.7 Hz)), which support the formation of a stable helical structure in solution.

Self-assembly of a tripodal building block $\mathbf{2}^{2+}$ via imine bond formation with a diamine linker, 1,3-propanediamine **5**, was investigated. 1,3-Propanediamine was selected for its appropriate length and relatively strong nucleophilicity as a primary amine. Considering the numbers of functional groups in $\mathbf{2}^{2+}$ and **5**, the resultant supramolecules would consist of a 2*n* number of $\mathbf{2}^{2+}$ and a 3*n* number of **5** (*n*; positive integer), respectively, when all the formyl groups and amine groups reacted.

Interestingly, the self-assembled products were dependent on the concentration of the components in solution. First, the ruthenium tripodand **2a**·$(PF_6)_2$ was mixed with the diamine **5** in a 2:3 ratio in $CDCl_3/CD_3CN$ = 1:1 at a low concentration, [$\mathbf{2a}^{2+}$] = 0.25 mM. The mixture was heated at 50 °C for 20 h to facilitate the formation of the Schiff base. A ^{1}H NMR spectrum after the reaction showed the disappearance of the formyl proton *a* at δ = 10.03 ppm and concomitant appearance of the imine proton *p* at δ = 8.33 ppm (Figure 3b). Upfield shifts of the protons of the paraphenylene group (*b* and *c*) also supported the reaction at the terminal formyl groups. ESI-TOF mass measurements of the sample gave signals assigned to $\mathbf{3a}^{4+}$, the Schiff base product formed from two tripodands $\mathbf{2}^{2+}$ and three diamines **5** (Figure S31). $\mathbf{3a}^{4+}$ is considered to have a macrobicyclic dimeric structure such as depicted in Figure 1b. Two structural isomers are possible for $\mathbf{3a}^{4+}$ depending on the relationship of the two Ru centers, i.e., *meso*-((Δ/Λ), (Λ/Δ)) and *rac*-((Δ/Δ), (Λ/Λ)). ^{1}H NMR indicated the formation of a single isomer. Protons of methylene group adjacent to the nitrogen (*q*) were observed as one triplet. For both *meso*- and *rac*-isomers, the two germinal protons (*q*) were chemically inequivalent, thus an overlap of the two signals was the case here. Examinations using PM3 calculations suggested that energy difference of *meso*- and *rac*- isomers are smaller than 1 kJ/mol (Figure S23). Thus, we were not able to conclude which isomer was formed.

Next, the self-assembly of **2**·$(PF_6)_2$ and **5** was performed at high concentration, [$\mathbf{2a}^{2+}$] = 5.0 mM, except where the condition was the same. The obtained ^{1}H NMR spectrum showed two sets

DOI: 10.1021/jacs.5b12752
J. Am. Chem. Soc. 2016, 138, 794−797

of signals for the tripodal unit (protons b–p) (Figure 3c). Signals that belong to one set (letters with subscript "1" and depicted in red in Figure 3c) were observed at similar chemical shifts to the macrobicyclic dimer **3a**·$(PF_6)_4$, while most of the other (letters with subscript "2" and depicted in blue) were shifted upfield. ESI-TOF mass spectrum gave signals assigned to $\mathbf{4a}^{8+}$, a Schiff base product formed from four $\mathbf{2a}^{2+}$ and six **5** and its PF_6^- adducts (Figure S31). Considering this stoichiometry and the ^{1}H NMR signal pattern, the resultant product at the high concentration was inferred to be the interlocked helicate **4a**·$(PF_6)_8$ composed of two macrobicyclic dimers.

The self-assembly process and the resultant products were further investigated from various aspects. Diffusion-ordered spectroscopy NMR of the sample in Figure 3c gave the same diffusion constant value $\log D = -9.2$ [$\log(m^2\ s^{-1})$] for all signals, which supports that a single species was formed at the 5.0 mM concentration (Figure S28). Analysis on concentration effect revealed that ratio of interlocked helicate **4a**·$(PF_6)_8$ against dimer **3a**·$(PF_6)_4$ increased with the concentration in the range of 0.25–5.0 mM (Figure S29). The concentration dependency on the ratio of $\mathbf{3a}^{4+}$ and $\mathbf{4a}^{8+}$ was not fit into a simple dimerization equilibrium model, which implies another factor involving the formation of **4a**·$(PF_6)_8$. ^{19}F NMR measurement of **4a**·$(PF_6)_8$ gave two sets of signals assigned to PF_6^- anions at $\delta = -65.9$ and -72.9 ppm (Figure S24). The signal at -72.9 ppm was ascribed to the free PF_6^- anions. From the signal intensities, the other one at -65.9 ppm was assigned to one PF_6^- anion encapsulated inside $\mathbf{4a}^{8+}$, which would have worked as a template to form the interlocked structure.[7,9f] The electrostatic interaction between an anionic PF_6^- and cationic $[Ru(bpy)_3]^{2+}$ parts would have worked as a driving force for the catenation. Further attempts to investigate the effect of the counteranions by exchanging PF_6^- with Cl^-, NO_3^-, BF_4^-, or TfO^- did not work well due to the low solubility of the $\mathbf{2a}^{4+}$ or $\mathbf{4a}^{8+}$ complexes in $CDCl_3$:CD_3CN = 1:1. The amount of the diamine **5** also affected the self-assembly process. The use of an excess amount (5 mol equiv) of **5** against **2a**·$(PF_6)_2$ did not lead to the imine bond formation but resulted in a cyclic aminal, the hexahydropyrimidine derivative (Figure S30).[18]

Detailed analysis by ^{1}H–^{1}H COSY and ^{1}H–^{1}H ROESY NMR together with molecular mechanics calculations unambiguously revealed its interlocked helical structure of **4a**·$(PF_6)_8$ (Figures S25 and S26). Full assignment of the ^{1}H NMR signals of **4a**·$(PF_6)_8$ is shown in Figure 3c. There were several indicative ROE correlations between the protons of two intercalated macrobicyclic units, such as (c_1–m_2), (d_1–l_2), and (f_1–n_2). Five kinds of diastereomers can be considered as intercalated tetramers, which are derived from the configurations around the metal centers, i.e., (ΔΔΔΔ), (ΔΔΔΛ), (ΔΔΛΔ), (ΔΛΔΛ), and (ΔΔΛΛ) (each one has an enantiomeric counterpart). Symmetry consideration based on the ^{1}H NMR spectrum, interunit ROE patterns (Figure 4b–d), and studies by molecular mechanics calculations (Figure 4a) lead us to conclude that **4a**·$(PF_6)_8$ had the (ΔΔΔΔ) (and its enantiomer) configurations, and the possibilities of the formation of the other isomers were excluded.

Comparison of the chemical shifts of the ^{1}H NMR signals of the tetramer **4a**·$(PF_6)_8$ and those of the dimer **3a**·$(PF_6)_4$ provided valuable information about the structure of **4a**·$(PF_6)_8$ (Table S2). The greatest upfield shift upon interlocking was observed for a benzylic proton j_2 ($\Delta\delta = -1.94$ ppm). This proton was positioned right above the para-phenylene linker of group 1 (depicted in red) in the molecular model, thus the shielding

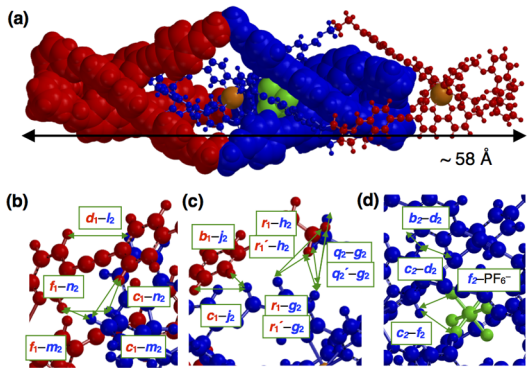

Figure 4. Structure of interlocked helicate $[(PF_6)@\mathbf{4a}]^{7+}$ obtained by molecular mechanics calculations. Ru atoms and a PF_6 anion are colored in orange and green, respectively. See Figure 3 for the other color coding. (a) The entire structure of the interlocked helicate optimized by molecular mechanics calculations (force field: MMFF). The crystal structure of **2a**·$(PF_6)_2$ was used as an initial structure of the tripodal parts. One dimeric unit, Ru atoms, and a PF_6^- anion are shown in a space-filling model. (b–d) Contact between interlocked structures (shown in a ball-and-stick model). Pairs of ^{1}H and ^{19}F were highlighted between which ROE or NOE peaks were observed. See also Figures S26 and S27.

effect from this aromatic ring is considered to be the reason for the large shift. As another aspect, the contribution of the C–H···π interaction between these moieties was expected. Other large upfield shifts (d_2 ($\Delta\delta = -1.36$ ppm), e_2 ($\Delta\delta = -1.03$ ppm), etc.) were also explained as the shielding effect from the interlocked counterpart. In contrast, the largest downfield shift was observed for f_2 ($\Delta\delta = +0.35$ ppm), a proton at the 6-position of the bipyridyl group. This is apparently peculiar, because most of the other protons that belonged to group 2 (depicted in blue) were upfield shifted. The downfield shift was ascribed to the hydrogen bonding with the encapsulated PF_6^- anion (C–H···F–P) that is positioned at the center of the interlocked structure (Figure 4a,d). The position of the PF_6^- was further confirmed by a ^{19}F–^{1}H heteronuclear NOE spectroscopy measurement, which exhibited correlations between proton f_2 and the encapsulated PF_6^- anion (Figure S27). Here, the hydrogen bonding together with the electrostatic interaction are considered to play an important role in the formation of the interlocked metallosupramolecular framework.[12b,f]

Moreover, it was indicated that the conformation of the central part of **4a**·$(PF_6)_8$ was literally "locked" as the result of catenation, even in its solution state. This became clear from the difference in the intraunit ROE correlation patterns of the diastereotopic methylene protons (j, j') and (q, q') for groups 1 and 2. Specifically, regarding the pairs of benzylic proton j and phenyl proton k, the ROE cross-peaks were both observed for group 1, (j_1–k_1) and (j_1'–k_1), while for group 2, only that of (j_2'–k_2) was detected (Figure S26). A similar discrimination existed for pairs of the imine proton p and methylene proton q.

By employing the Fe tripodal unit **2b**·$(BF_4)_2$ or **2b**·$(PF_6)_2$, the isostructural interlocked helicates **4b**·$(BF_4)_8$ and **4b**·$(PF_6)_8$ were also formed, respectively (Figures S32 and 33). The tripodal motif $\mathbf{2}^{4+}$ is a characteristic feature of the hierarchical self-assembled system. When the ligand **1**, $Fe(BF_4)_2$, and diamine **5** were mixed altogether instead of using **2b**·$(BF_4)_2$, the interlocked tetramer **4b**·$(BF_4)_8$ was not obtained, but the complexation between the diamine **5** and $Fe(BF_4)_2$ took place (Figure S34). The use of $\mathbf{2}^{4+}$ is beneficial not only for the construction of large self-assembled structures but also for the recovery of starting

DOI: 10.1021/jacs.5b12752
J. Am. Chem. Soc. 2016, 138, 794–797

materials. By treating **4a**·$(PF_6)_8$ with H^+, the imine bond was hydrolyzed, and the monomeric **2a**·$(PF_6)_2$ was recovered (Figure S35). These features would have not been achieved by the helicate structures constructed by the direct complexation of metal ions and linear ligands with multiple binding sites,[9a,g,13d] thus showing the usefulness of the preorganized tripodal building block.

In conclusion, a tripodal helical complex unit $\mathbf{2}^{2+}$ composed of the ligand **1** and octahedral metal centers (M^{II} = Ru^{II} and Fe^{II}) were synthesized. The self-assembly via imine bond formation of the three formyl groups of **2**·$(PF_6)_2$ and 1,3-propanediamine **5** resulted in the formation of two products, the macrobicyclic dimer $\mathbf{3}^{4+}$ and interlocked helicate $\mathbf{4}^{8+}$, depending on the concentration. The rigid ethenylphenyl linker introduced into **1** afforded a large inner space upon the formation of the supramolecular structure, which enabled the catenation of the large tripodal units. A detailed analysis of the solution structure of **4a**·$(PF_6)_8$ revealed that the effective conformation control of the triple-stranded helical structures with a length up to 58 Å was achieved. The interlocked motif could be further extended into helical polymers by modifying the tripodal part into a Janus-type, bidirectional structure. In another aspect, molecular recognition functions can be installed into the tripodal units,[12a,14] which would realize, in combination with this interlocked linear motif, the allosteric regulation based on the long-range transmittance of the structural information.

■ ASSOCIATED CONTENT

Supporting Information

The Supporting Information is available free of charge on the ACS Publications website at DOI: 10.1021/jacs.5b12752.

Detailed synthetic procedures, characterization data, 1D and 2D NMR measurements (PDF)
Crystallographic data (CIF)

■ AUTHOR INFORMATION

Corresponding Author

*nabesima@chem.tsukuba.ac.jp

Notes

The authors declare no competing financial interest.

■ ACKNOWLEDGMENTS

This research was financially supported by Grants-in-Aid for Scientific Research from the Ministry of Education, Culture, Sports, Science, and Technology of Japan.

■ REFERENCES

(1) Fratzl, P.; Weinkamer, R. *Prog. Mater. Sci.* **2007**, *52*, 1263.
(2) Woodcock, C. L.; Dimitrov, S. *Curr. Opin. Genet. Dev.* **2001**, *11*, 130.
(3) (a) Hof, F.; Craig, S. L.; Nuckolls, C.; Rebek, J., Jr. *Angew. Chem., Int. Ed.* **2002**, *41*, 1488. (b) Fujita, M.; Tominaga, M.; Hori, A.; Therrien, B. *Acc. Chem. Res.* **2005**, *38*, 371. (c) Chakrabarty, R.; Mukherjee, R.; Stang, P. J. *Chem. Rev.* **2011**, *111*, 6810.
(4) Amabilino, D. B.; Stoddart, J. F. *Chem. Rev.* **1995**, *95*, 2725.
(5) Balzani, V.; Credi, A.; Raymo, F. M.; Stoddart, J. F. *Angew. Chem., Int. Ed.* **2000**, *39*, 3348.
(6) Kremer, C.; Lützen, A. *Chem. - Eur. J.* **2013**, *19*, 6162.
(7) (a) Freye, S.; Michel, R.; Stalke, D.; Pawliczek, M.; Frauendorf, H.; Clever, G. H. *J. Am. Chem. Soc.* **2013**, *135*, 8476. (b) Löffler, S.; Lübben, J.; Krause, L.; Stalke, D.; Dittrich, B.; Clever, G. H. *J. Am. Chem. Soc.* **2015**, *137*, 1060.
(8) (a) Vickers, M. S.; Beer, P. D. *Chem. Soc. Rev.* **2007**, *36*, 211. (b) Harada, A.; Hashidzume, A.; Yamaguchi, H.; Takashima, Y. *Chem. Rev.* **2009**, *109*, 5974. (c) Van Dongen, S. F. M.; Cantekin, S.; Elemans, J. A. A. W.; Rowan, A. E.; Nolte, R. J. M. *Chem. Soc. Rev.* **2014**, *43*, 99. (d) Chen, Q.; Chen, L.; Jiang, F.; Hong, M. *Chem. Rec.* **2015**, *15*, 711.
(9) (a) Fukuda, M.; Sekiya, R.; Kuroda, R. *Angew. Chem., Int. Ed.* **2008**, *47*, 706. (b) Westcott, A.; Fisher, J.; Harding, L. P.; Rizkallah, P.; Hardie, M. J. *J. Am. Chem. Soc.* **2008**, *130*, 2950. (c) Li, F.; Clegg, J. K.; Lindoy, L. F.; Macquart, R. B.; Meehan, G. V. *Nat. Commun.* **2011**, *2*, 205. (d) Langton, M. J.; Matichak, J. D.; Thompson, A. L.; Anderson, H. L. *Chem. Sci.* **2011**, *2*, 1897. (e) Ponnuswamy, N.; Cougnon, F. B. L.; Clough, J. M.; Pantos, G. D.; Sanders, J. K. M. *Science* **2012**, *338*, 783. (f) Zhu, R.; Lübben, J.; Dittrich, B.; Clever, G. H. *Angew. Chem., Int. Ed.* **2015**, *54*, 2796. (g) Gidron, O.; Jirásek, M.; Trapp, N.; Ebert, M.-O.; Zhang, X.; Diederich, F. *J. Am. Chem. Soc.* **2015**, *137*, 12502.
(10) (a) Borisova, N. E.; Reshetova, M. D.; Ustynyuk, Y. A. *Chem. Rev.* **2007**, *107*, 46. (b) Mastalerz, M. *Angew. Chem., Int. Ed.* **2010**, *49*, 5042. (c) Belowich, M. E.; Stoddart, J. F. *Chem. Soc. Rev.* **2012**, *41*, 2003.
(11) (a) Jedrzejewska, H.; Wierzbicki, M.; Cmoch, P.; Rissanen, K.; Szumna, A. *Angew. Chem., Int. Ed.* **2014**, *53*, 13760. (b) Li, H.; Zhang, H.; Lammer, A. D.; Wang, M.; Li, X.; Lynch, V. M.; Sessler, J. L. *Nat. Chem.* **2015**, *7*, 1003.
(12) (a) Nabeshima, T. *Bull. Chem. Soc. Jpn.* **2010**, *83*, 969. (b) Beves, J. E.; Blight, B. A.; Campbell, C. J.; Leigh, D. A.; McBurney, R. T. *Angew. Chem., Int. Ed.* **2011**, *50*, 9260. (c) Vigato, P. A.; Peruzzo, V.; Tamburini, S. *Coord. Chem. Rev.* **2012**, *256*, 953. (d) Nabeshima, T.; Yamamura, M. *Pure Appl. Chem.* **2013**, *85*, 763. (e) Frischmann, P. D.; MacLachlan, M. J. *Chem. Soc. Rev.* **2013**, *42*, 871. (f) Smulders, M. M. J.; Riddell, I. A.; Browne, C.; Nitschke, J. R. *Chem. Soc. Rev.* **2013**, *42*, 1728.
(13) (a) Ayme, J.-F.; Beves, J. E.; Leigh, D. A.; McBurney, R. T.; Rissanen, K.; Schultz, D. *Nat. Chem.* **2012**, *4*, 15. (b) Young, M. C.; Holloway, L. R.; Johnson, A. M.; Hooley, R. J. *Angew. Chem., Int. Ed.* **2014**, *53*, 9832. (c) Faulkner, A. D.; Kaner, R. A.; Abdallah, Q. M. A.; Clarkson, G.; Fox, D. J.; Gurnani, P.; Howson, S. E.; Phillips, R. M.; Roper, D. I.; Simpson, D. H.; Scott, P. *Nat. Chem.* **2014**, *6*, 797. (d) Wood, C. S.; Ronson, T. K.; Belenguer, A. M.; Holstein, J. J.; Nitschke, J. R. *Nat. Chem.* **2015**, *7*, 354.
(14) (a) Nabeshima, T.; Yoshihira, Y.; Saiki, T.; Akine, S.; Horn, E. *J. Am. Chem. Soc.* **2003**, *125*, 28. (b) Nabeshima, T.; Tanaka, Y.; Saiki, T.; Akine, S.; Ikeda, C.; Sato, S. *Tetrahedron Lett.* **2006**, *47*, 3541. (c) Nabeshima, T.; Masubuchi, S.; Taguchi, N.; Akine, S.; Saiki, T.; Sato, S. *Tetrahedron Lett.* **2007**, *48*, 1595.
(15) (a) Manabe, K.; Okamura, K.; Date, T.; Koga, K. *J. Org. Chem.* **1993**, *58*, 6692. (b) Abe, H.; Horii, A.; Matsumoto, S.; Shiro, M.; Inouye, M. *Org. Lett.* **2008**, *10*, 2685.
(16) (a) Mann, S.; Huttner, G.; Zsolnai, L.; Heinze, K. *Angew. Chem., Int. Ed. Engl.* **1996**, *35*, 2808. (b) Yasuda, M.; Nakajima, H.; Takeda, R.; Yoshioka, S.; Yamasaki, S.; Chiba, S.; Baba, A. *Chem. - Eur. J.* **2011**, *17*, 3856.
(17) (a) Weizman, H.; Libman, J.; Shanzer, A. *J. Am. Chem. Soc.* **1998**, *120*, 2188. (b) Fletcher, N. C.; Nieuwenhuyzen, M.; Prabarahan, R.; Wilson, A. *Chem. Commun.* **2002**, 1188. (c) Ulrich, G.; Bedel, S.; Picard, C. *Tetrahedron Lett.* **2002**, *43*, 8835. (d) Fletcher, N. C.; Brown, R. T.; Doherty, A. P. *Inorg. Chem.* **2006**, *45*, 6132. (e) Oyler, K. D.; Coughlin, F. J.; Bernhard, S. *J. Am. Chem. Soc.* **2007**, *129*, 210. (f) Fletcher, N. C.; Martin, C.; Abraham, H. J. *New J. Chem.* **2007**, *31*, 1407. (g) Sato, K.; Sadamitsu, Y.; Arai, S.; Yamagishi, T. *Tetrahedron Lett.* **2007**, *48*, 1493. (h) Pintér, Á.; Haberhauer, G. *Eur. J. Org. Chem.* **2008**, *2008*, 2375. (i) Baker, N. C. A.; Fletcher, N. C.; Horton, P. N.; Hursthouse, M. B. *Dalton Trans.* **2012**, *41*, 7005. (j) Hao, Y.; Yang, P.; Li, S.; Huang, X.; Yang, X.-J.; Wu, B. *Dalton Trans.* **2012**, *41*, 7689.
(18) Locke, J. M.; Griffith, R.; Bailey, T. D.; Crumbie, R. L. *Tetrahedron* **2009**, *65*, 10685.

DOI: 10.1021/jacs.5b12752
J. Am. Chem. Soc. 2016, 138, 794−797